www.czasopisma.pan.pl PAN POLSKA AKADEMIA NAUK www.journals.pan.pl

PAN ARCHIVES OF ACOUSTICS
Vol. **39**, No. 4, pp. 427–438 (2014)

DOI: 10.2478/aoa-2014-0047

Review Papers

Ultrasonic Synthetic Apertures: Review

Andrzej NOWICKI, Barbara GAMBIN

Institute of Fundamental Technological Research
Polish Academy of Sciences
Pawińskiego 5B, 02-106 Warszawa, Poland; e-mail: {anowicki, bgambin}@ippt.pan.pl

(*received June 16, 2014; accepted November 24, 2014*)

In the paper the concept of synthetic aperture used for high resolution/high frame rate ultrasonic imaging is reviewed. The synthetic aperture technique allows building extended "virtual" apertures, synthesized from smaller real aperture resulting in improved lateral resolution along full penetration depth without sacrificing the frame rate.

Especially, four methods, synthetic aperture focusing (SAF), multi-element synthetic aperture focusing (M-SAF), synthetic receive aperture (SRA) and synthetic transmit aperture (STA) are addressed. The effective aperture function, describing two-way, far field radiation is a useful tool in beam pattern analysis. Some basic notations, which are used to calculate the effective aperture are introduced in Appendix.

Keywords: synthetic aperture, effective aperture, ultrasonography.

1. Introduction

In the early 1950s, the Synthetic Aperture Radar SAR was first developed as a military reconnaissance device. Almost 50 years later the achievements in signal processing and array transducers allowed to transfer the main basic ideas of SAR the field of ultrasonic real time medical imaging.

The standard scanning ultrasonic technique is based on delay and sum (DAS) processing, both on transmitting and receiving side in order to achieve the required beam forming. The beam shape is a crucial for imaging resolution. The scanning beam can be focused (within the near field) on specific depth by applying a proper time steering to the individual transducers in linear array. Outside of the focal length the lateral resolution deteriorates substantially. Modern US scanners allow for multi focusing, however at the cost of decreasing frame rate *FR*. The *FR* is inversely proportional to the number of chosen focal zones M, $FR \propto 1/M$. The length of the focal zone is proportional to the depth of the focal field $r|_D$.

For constant f-number ($f_\# = \text{const}$) the useful depth of imaging field $\sum r|_D$ covering all M focal zones is given by

$$\sum_M r|_D = M \cdot r|_D. \tag{1}$$

The *FR* limitation can be omitted by applying the synthetic aperture arrays. The radar systems of imaging of the earth's surface have been using the method of synthetic aperture SA, as an effective alternative to large, multi-antenna radar. Instead of increasing the aperture of antennas in order to improve the lateral resolution, the similar effect is obtained by the transmitting the probing signals, and then providing the synthesis of the echoes from the individual antenna elements. The concept of SAR is now increasingly being implemented in the ultrasound.

Consider the case where the actual aperture D is divided into non-overlapping N_s subaperture with size $D_s = D/N_s$. Each subaperture D_s can be pre-focused at depth F_D and its useful range $r|_{D-SA}$ is

$$r|_{D-SA} = \lambda(F_D/D_s)^2 = (N_s)^2\lambda(F_D/D)^2, \tag{2}$$

where λ is wavelength of the transmitted pulse.

The resulting depth of field is

$$r|_{D-SA} = \lambda(F_D/D_s)^2 = (N_s)^2 r|_D.$$

Thus N_s pulses synthetic aperture mode gives the same depth as the N_S^2 pulses in a standard linear array beam forming. Clearly, the speed of image formation increases N_s times (Jensen *et al.*, 2006).

The study focused on ultrasonic applications of synthetic apertures already started in the late sixties (Flaherty *et al.*, 1967; Burckhardt *et al.*, 1974). The flexible of-line processing for SA data analysis was also addressed by Trots *et al.* (2008). The algorithm

allowing considerable reduction of the data acquisition for SA image reconstruction was proposed by Karwat *et al.* (2010). Kortbek *et al.* (2013) proposed a novel approach to SA using virtual sources and virtual receivers dynamically expanded the array size and allowing dynamic focusing in both transmit and receive. The SAFT technique was considerably improved applying focusing beam before image (Mosey *et al.*, 2013). An interesting enhancement of SA imaging was proposed by Hansen and Jensen (2012). The authors investigated the compound imaging with convex arrays for any number of angles without reducing the frame rate or temporal resolution. The degradation of image quality close to a virtual source was addressed by Kim *et al.* (2012). Authors introduced the dynamic SA where the number of synthetic scan lines for acoustic field superposition is dynamically adjusted based on the transmit acoustic field analysis.

Among the many systems implementing the synthetic apertures, the most often used are:

- Synthetic Aperture Focusing – SAF. In this system, the single element is transmitting the scanning pulse and next is receiving the echoes. The sequence is repeating N times where N is the number of individual transducers in the array. Echoes are stored in the system memory and then processed to produce an image of the scanned area. Frame rate increases significantly, however the contrast dynamics decreases since the individual array transducers emit low energy and signal/noise ratio SNR decreases. The required memory of the system is high.
- Multi-element Synthetic Aperture Focusing M-SAF. The transmitting and receiving transducers are grouped, which can significantly increase energy and improve the SNR. The focusing is performed at all depths providing the very high frame rate. Rather high memory of the system is required (as in SAF).
- Synthetic Transmit Aperture STA. In this method the individual array transducers (or groups of them, just as in M-SAF) transmit the scanning pulses, and then all the elements of the array receive the echoes. Focusing is realized in both processes, transmitting and receiving while maintaining high *FR*. Very large memory for data acquisition is required. In a standard beam forming array with N elements, N data "lines" for each array element involved in the formation of the image line. $N \times N$ data have to be memorized in order to effectively synthesize the image. If the transmitting apertures are consisting K elements then the size of required memory decreases proportionally to N/K. A certain modification of the STA is the choice of sparse transmitting matrix.
- Synthetic Receive Aperture SRA. The lateral resolution is direct function of the size of the transmitting/receiving aperture. While the formation of the transmit aperture is relatively simple and not aggravating the calculation process, the manipulation of the length of the receiving sequence is complex and computationally expensive. The SRA systems proposed in the literature (Nock, Trahey, 1992; Walker, Trahey, 1994) use rather large transmitting apertures. While the receiving apertures are divided into smaller subapertures. Each image line is formed in the following sequence – single transmission for each receiving subaperture. For one probing pulse sent from full transmitting aperture the RF echoes from all transducers in receiving subapertures are summed and then stored in memory. After storing the complete sequence of transmission – reception sequences the final image is reconstructed.

2. The effective aperture in the far field

Let us introduce the concept of effective aperture as the equivalent aperture used in the classical beam forming (Chiao, Thomas, 1996; Lockwood, Foster, 1995).

Let the linear array consists of N sources with apodization function $w(n)$, $n = 0, 1, \ldots, N-1$.

The weighted transmitting or receiving aperture $\mathbf{w} \equiv [w(0), w(1), ..., w(N-1)]$ is the matrix with dimension N.

The shape of the beam in the far field has the form:

$$W_T(\theta) = \sum_{n=0}^{N-1} w(n) e^{-ndk \sin\theta}, \tag{3}$$

where k is the wave number, θ is a beam angle and d is equal to the array pitch.

The discrete Fourier transform (DFT) of the weighted transmitting or receiving aperture $\mathbf{w}$ is equal to

$$\mathrm{DFT}\{\mathbf{w}\} \equiv W(i) = \sum_{n=0}^{N-1} w(n) e^{-j\frac{2\pi}{N}in}, \quad i = 0, 1, ..., N-1. \tag{4}$$

Index i represents the number of the spectral line and it transforms into the beam angle θ according to the relationship $\sin\theta = i\lambda/Nd$. The angle θ was replaced by N discrete samples. If N elements array is regarded as a single period of the function then the DFT transforms the periodic array into N samples with the sample distance $\lambda/(Nd)$. If the distance between the discrete samples of the function $W(\theta)$ is $\Delta\theta$ in the domain of the spatial angle and Δd in respect to the aperture then $m\Delta\theta$ and $i\Delta d$ are respectively equivalent to the angle and aperture (by analogy to the signals in the frequency and time domain).

The beam pattern in the far field can be calculated using Fourier transform of the source aperture.

The shape of the effective transmitting-receiving beam is equal to the product of transmit and receive beams:

$$W_{TR}(\theta) = W_T(\theta) \cdot W_R(\theta). \tag{5}$$

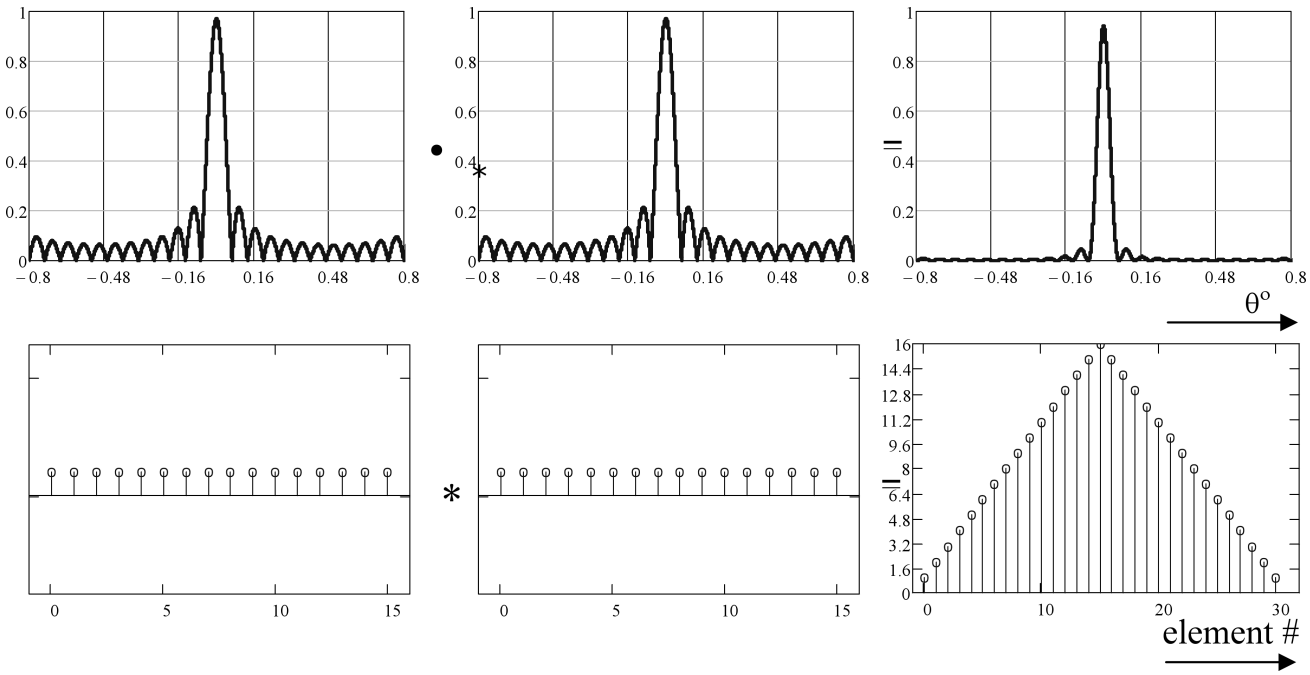

Fig. 1. The effective aperture of the transmitting - receiving aperture for 16 elements phase array with the apodization functions $w_T(n) = w_R(n) = 1$. At three lower drawings the array elements are marked – from left to right: transmitting array ($N = 16$), receiving array ($N = 16$) and the convolution of both being the effective aperture ($N_{\text{eff}} = 2N-1 = 31$). Upper three plots correspond to, from left to right: the transmitted beam pattern, the receiving beam pattern and their product being the effective beam pattern.

From the properties of the Fourier transform, we know that the product of the transforms of two functions is equal to the transform of the convolution of these functions,

$$W_{TR}(n) = \text{DFT}[\mathbf{w}_T * \mathbf{w}_R](n), \tag{6}$$

where $n = 1, 2, ..., 2N-1$.

The convolution $(\mathbf{w}_T * \mathbf{w}_R)(n)$ is called the effective aperture $AP_{\text{eff}}(n)$.

The construction of the effective aperture for 16 elements linear array is shown in Fig. 1.

From Fig. 1 we clearly see that the effective aperture for a uniform apodization of N transmitting and receiving transducers has a length $2N-1$ elements apodized according to the triangular function (Bartlett window) with amplitude corresponding to the number of overlapping and then summed (convolution) pairs – of transmitting and receiving transducers. This is characteristic shape of the effective apertures for linear arrays, e.g. phase arrays.

The total number of elementary sources n_{TR} in the effective aperture $AP_{\text{eff}}(n)$ is equal to $n_{TR} = n_T + n_R - 1$, where n_T and n_R are the number of elementary sources transmitting and receiving, respectively.

In summary, the matrix of effective transmitting-receiving array aperture matrix $\mathbf{w}_{TR}$ is equal to the product (outer product) of transmit apodization matrix $\mathbf{w}_T$ and transpose receiving apodization matrix $\mathbf{w}_R^T$, cf. Appendix. The matrix $\mathbf{w}_{TR}$ is a square matrix $N \times N$. The rows correspond to the transmitting elements and columns are the receiving elements:

$$\begin{aligned} \mathbf{w}_{TR} &= [w_{TR}(i,j)], \\ \mathbf{w}_{TR}(i,j) &= w_T(i) w_R(j), \\ i,j &= 1, 2, ..., N-1. \end{aligned} \tag{7}$$

The matrix $\mathbf{w}_{TR}$ enables the efficient optimization of the aperture. Each element of the matrix corresponds to a pair of transmitter-receiver with the value for this position of being the product of weights for transmit and receive.

The effective aperture is defined as the convolution of both aperture functions, transmitting and receiving.

$$AP_{\text{eff}}(n) = (\mathbf{w}_T * \mathbf{w}_R)(n). \tag{8}$$

3. Synthetic Aperture Focusing – SAF

As already mentioned, the simplest system is a synthetic focusing aperture SAF, first described in ultrasound applications by O'Donnell and Thomas (1992). In SAF system only single element is active during transmit-receive sequence and after each sequence the transmit-receive pair id shifted by one pitch. Transmission and reception sequence is repeated N times, so many times as the number of elements in the entire array, see Fig. 2.

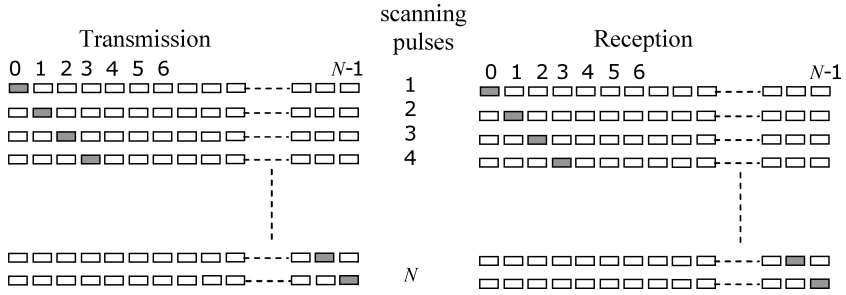

Fig. 2. Transmitting and receiving strategy in SAF.

If each source is small enough then it creates a spherical wave front, propagating through the medium. On the receive side, for each subsequent transmission, the same transducer (or all transducers in the array) is activated recording the echoes – at this stage the image is synthesized only during reception corresponding to the process of dynamic focusing, and therefore the resulting resolution is rather low. After successive transmissions until the last element of the linear array was activated and acquisition of the echoes' matrix all stored echoes are coherently summed, yielding an image with high resolution, dynamically focused during transmission and reception.

Focusing using SAF follows a similar approach as in a standard beam forming using Delay and Sum (DAS) algorithm, however the complexity of the system is by far smaller because only one transmit-receive circuitry is required, see Fig. 3.

The difference in the round trip time from the n-th transducer to the point P and back to the center of the array is

$$\tau_n = 2\frac{(R_c - R_n)}{c}, \tag{9}$$

where c is the sound speed and

$$R_n = \sqrt{y_n^2 + R_c^2 - 2y_n R_c \sin\theta}. \tag{10}$$

After replacing y_n with the distance from the center of the array counted in discrete steps, we have:

$$y_n = \left[-\left(\frac{N-1}{2} - n\right)d\right] \tag{11}$$

and Eq. (9) takes a form

$$\tau_n = \frac{1}{c}\left[R_c - \sqrt{[-(a^*)d]^2 + R_c^2 - 2(b^*)dR_c\sin\theta}\right], \tag{12}$$

where

$$a^* = \frac{N-1}{2} - n, \qquad b^* = -\frac{N-1}{2} - n.$$

The part of the delay required for beam deflection is equal

$$\tau_n^\theta = \frac{-2\left(\frac{N-1}{2} - n\right)d\sin\theta}{c}. \tag{13}$$

In the far field, we can skip the delay associated with the focusing and for any point $P(R,\theta)$ the echo line $A(R,\theta)$ has the form

$$A_{SAF}(R,\theta) = \sum_{n=0}^{N-1} e_n(t-\tau_n) = \sum_{n=0}^{N-1} e_n\left(\frac{R_n}{c} - \tau_n\right), \tag{14}$$

where $e_n(t)$ is the echo data recorded by n-th transducer in the array.

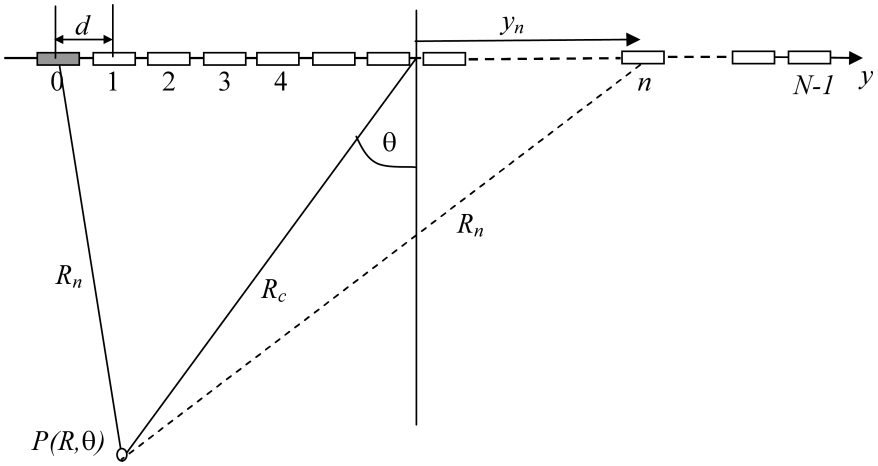

Fig. 3. Linear array geometry for transmission and acquisition in SAF.

In the far field the beam shape is described by the formulas:

$$W_{SAF}(R,\theta) = \sum_{n=0}^{N-1} e^{-j\omega\tau_n^{\theta}} = \sum_{n=0}^{N-1} e^{-jk2\left(-\frac{N-1}{2}+n\right)d\sin\theta}, \quad (15)$$

$$|W_{SAF}(R,\theta)| = \frac{\sin\left(kNd\sin\left(\theta\right)\right)}{\sin\left(kd\sin\left(\theta\right)\right)}.$$

The Eq. (15) is relatively simple being the sum of subsequent products of transmitting matrix and transposed receiving matrix.

Effective aperture for SAF system may be calculated from the formula:

$$AP_{\text{eff}}(i) = \sum_{n=1}^{N} (\mathbf{w}_T^n * \mathbf{w}_R^n)(i), \quad i = 1, ..., 2N-1, \quad (16)$$

where $\mathbf{w}_T^n = \mathbf{w}_R^n = [0, \ldots, 0, A_n, 0, \ldots, 0]$ with apodization $A_n = 1$, upper indices correspond to the number of successive transmission/reception.

The effective aperture has the length of $2N-1$ but with only N-active sources distant from each by twice the distance d (pitch) compared to the actual distance d between the elements of the array. This results in the changed position of the gratings lobes compared to the radiation field of identical transmit-receive aperture in DAS beam forming system.

The simplify scheme of calculating the effective aperture for eight elements array is shown in Fig. 4. The corresponding far field transmitting/receiving beam pattern comparing the eight elements SAF and phase array, for different array pitch is shown in Fig. 5.

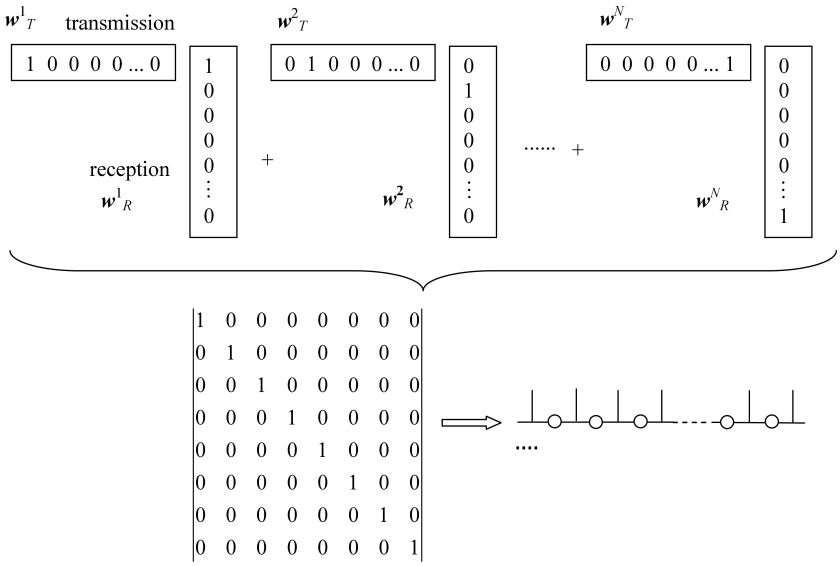

Fig. 4. Computing the effective aperture of an array with eight elements.

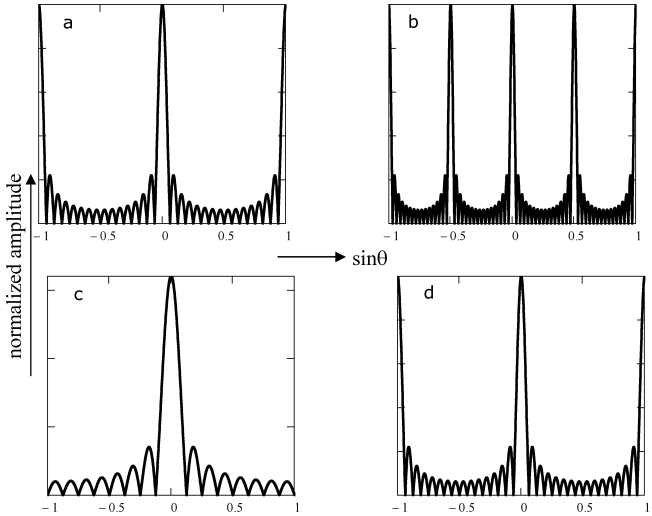

Fig. 5. The transmit/receive far field beam pattern for 8 elements array, a) phase array, $d = 1.2\lambda$, b) SAF, $d = 1.2\lambda$, c) phase array $d = 0.5\lambda$, d) SAF, $d = 0.5\lambda$. The distance between grating lobes for SAF two times shorter (Eq. (15)) than for the phase array beam forming.

The distance between the centers of the sources for SAF effective aperture is doubled. So, if the pitch in linear array was equal to $\lambda/2$ then the effective distance between centers of elements in SAF is twice as long being equal λ.

The comparison of SAF and phase array radiation fields shows that while the width of the main lobe (and thus the lateral resolution) is improved but the grating lobes are clearly appearing due to not sufficiently dense spatial sampling ($d > \lambda/2$). For SAF the width of scanning at -6 dB is $W_{SAF-6\,\mathrm{dB}} \approx 0.33\lambda/L$ while for phase array $W_{ph-6\,\mathrm{dB}} \approx 0.44\lambda/L$, where $L = N \cdot d$.

Since only one element of the array transmits a scanning pulse and next receives the echoes, so the energy efficiency of SAF decreases significantly. Also the contrast dynamics is worsening due to the higher level of side lobes.

4. Multi-element Synthetic Aperture Focusing M-SAF

For N-elements array, in which only one source is active during transmission and reception, signal/noise ratio decreases $10\log(N)$ times compared with a phase array. For example for 128 transducers phase array the signal/noise ratio is up to 21 dB greater than for SAF comprising of the same number of transducers. Currently, standard SAF are rather not used, instead, they modified in a way that the individual sources are replaced by multi- subapertures. Such systems are called Multi-element Synthetic Aperture Focusing M-SAF. Compared to SAF, they transmit higher ultrasonic energy. Ylitalo (1996) showed that the signal/noise ratio for M-SAF can be up $10\log(K \cdot K)$ higher than for SAF, where K is the number of sources in transmitting and receiving subapertures. The energy gain for 8-elements subapertures is close to 18 dB.

In practice, the gain is not that high when the subapertures are larger then the beam gets narrower and do not illuminate the entire image space. The M-SAF algorithm is basically identical to the one of SAF. The difference lies in the fact that instead of single element transmission/reception, the K_T and K_R subapertures are used during transmission and reception, respectively, (Karaman *et al.*, 1995; 1998). In practice both, transmit and receive subapertures are set to have the same length, $K_T = K_R = K$. The subsequent transmitting and receiving pairs are shifted along the array by one or more elements. The number of non-overlapping subapertures is equal $S = int(N/K)$.

Theoretically, the transmitting subaperture in M-SAF should radiate a spherical wave front, similarly to a small source. However for $K_T \leq 12$ the transmitted beam does not deviate much from the distribution the field generated by a single source (Karaman *et al.*, 1998).

Effective aperture for M-SAF system can be calculated from the formula

$$AP_{\mathrm{effM\text{-}SAF}}(i) = \sum_{n=1}^{N-K+1} \left(\mathbf{w}_T^n * \mathbf{w}_R^n\right)(i), \qquad i = 1, ..., 2N-1, \tag{17}$$

wherein, in the case of the same subapertures used in the process of transmission and reception, $\mathbf{w}_T^n = \mathbf{w}_R^n = [0, \ldots, 0, A_n, A_{n+1}, \ldots, A_{n+K-1}, 0, \ldots, 0]$. With no apodization $A_n = A_{n+1} = \ldots = A_{n+K-1} = 1$ and the effective aperture is equal to $2N-K$.

The far field has the form

$$\begin{aligned} W_{\mathrm{M\text{-}SAF}}(R,\theta) &= \sum_{i=0}^{N-K_R} \sum_{m=0}^{K_R-1} e^{-j\omega\left(\tau_{m+i}^{\theta} - \tau_i^{\theta}\right)} \\ &= e^{jk\frac{N-1}{2}d\sin\theta} e^{jk\frac{N-K_R}{2}d\sin\theta} \\ &\quad \sum_{i=0}^{N-K_R} e^{-jki2d\sin\theta} \\ &\quad \sum_{m=0}^{K_R-1} e^{-jkmd\sin\theta}. \end{aligned} \tag{18}$$

Indices m and n will correspond to the position of transmitting and receiving transducer/subaperture, respectively.

Summing after the transmitting subapertures can be omitted because we can consider it roughly like

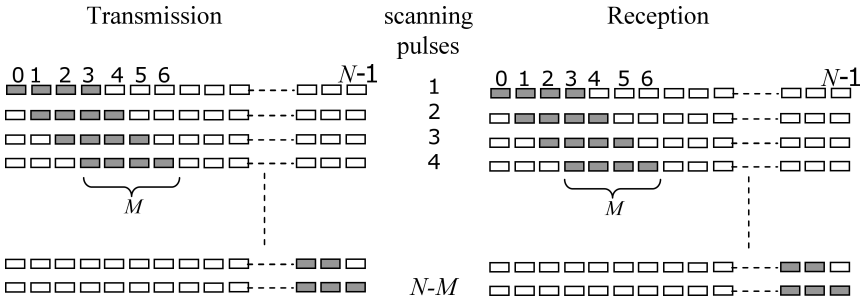

Fig. 6. Transmitting and receiving strategy for M-SAF, $K_T = K_R = 4$.

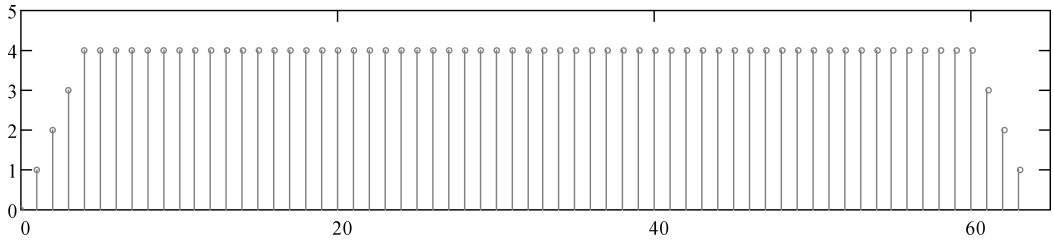

Fig. 7. Effective aperture of 32 elements M-SAF and $K_T = K_R = 4$ shifted by full length of subapertures (four elements).

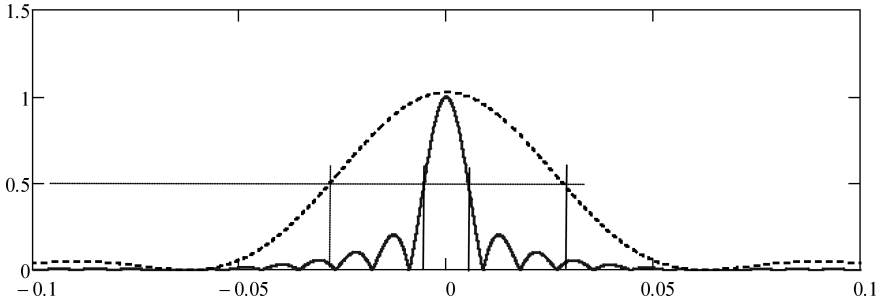

Fig. 8. Far field response for 32 elements; solid line M-SAF with $K_T = K_R = 4$ shifted by full length of subapertures (four elements), dashed line – phase array. Lateral resolution for M-SAF is roughly 5 times better.

a small point source. Equation (18) can be written in the form

$$|W_{\text{M-SAF}}(R,\theta)| = \frac{c^*}{\sin(kd\sin\theta)\sin\left(k\frac{d}{2}\sin\theta\right)}, \quad (19)$$

where

$$c^* = \sin\left(k\left(N-K_R+1\right)d\sin\theta\right)\sin\left(kK_R\frac{d}{2}\sin\theta\right).$$

The first term is identical to SAF with $N-K_R+1$ elements. The second term modifies the field due to the receiving aperture with K_R elements. This term decreases both, the gratings and side lobes generated by subaperture $N-K_R+1$ long.

M-SAF can be modified by shifting the subapertures by their full length K without partial overlapping and without pre-focusing on the transmitting side. Then the far field beam is given by

$$\begin{aligned} W_{\text{M-SAF}}(\theta) &= \sum_{i=0}^{S-1}\sum_{m=0}^{K_T-1}\sum_{n=0}^{K_R-1} e^{j\omega(\tau_{i,m}+\tau_{i,m})} \\ &= e^{jk\frac{N-1}{2}2d\sin\theta}\sum_{i=0}^{S-1} e^{jki2K_Td\sin\theta} \\ &\quad \sum_{m=0}^{K_T-1} e^{jkmd\sin\theta}\sum_{n=0}^{K_R-1} e^{jknd\sin\theta}, \end{aligned} \quad (20)$$

$$|W_{\text{M-SAF}}(\theta)| = \frac{\sin\left(kSK_Td\sin\theta\right)}{\sin\left(kK_Td\sin\theta\right)} \cdot \left[\frac{\sin\left(kK_T\frac{d}{2}\sin\theta\right)}{\sin\left(k\frac{d}{2}\sin\theta\right)}\right]^2.$$

The first term is identical to SAF with transmit aperture of length $L = SK_Td$ sampled at subaperture K_T. If 50% of subapertures will overlap one on each other then the grating lobes will disappear.

The effective aperture for M-SAF array consisting 32 sources activated in sequences of four non-overlapping transmitting elements and four receiving elements is shown in Fig. 7. The corresponding pressure far field is shown in Fig. 8. It clear that the resulting lateral resolution in the far field is much better for M-SAF than for the standard phase array system.

5. Synthetic Receiving Aperture SRA

In this section we will discuss the synthetic aperture in the form of a linear array in which all elements of the array are activated at the same time (Trahey, Nock, 1992a; 1992b). Large transmitting aperture translates into narrow beam resulting in improved lateral resolution While it is relatively ease to address all array transmitting elements, addressing and memorizing echoes lines from a large receiving aperture is rather computationally intensive task.

The acquisition of echoes is as follows. The transmitter activates all sources of transmitting aperture simultaneously for each subsequent receiving subaperture. Reconstruction of an image line requires summing of all echoes from receiving subaperture and storing the resulting matrix in the system memory. The number of transmissions for a single imaging sequence is equal to the number of subapertures. After storing of all signals they are coherently summed for the reconstruction of the full imaging sector.

For the N-elements array of the receiving aperture is divided into $S = N/K_R$ receiving subapertures K_R length each.

The far field beam is given by

$$W_{SAR}(\theta) = \sum_{m=0}^{N-1}\sum_{i=0}^{S-1}\sum_{n=0}^{K_R-1} e^{-j\omega\left(\tau^{\theta}_{K_R+n}+\tau^{\theta}_{m}\right)}$$

$$= e^{jk(N-1)d\sin\theta}\sum_{m=0}^{N-1} e^{jkmd\sin\theta}$$

$$\sum_{i=0}^{S-1} e^{-jkiK_Rd\sin\theta}$$

$$\sum_{m=0}^{K_R-1} e^{-jknd\sin\theta}, \tag{21}$$

$$|W_{SAR}(\theta)| = \frac{\sin\left(k\frac{Nd}{2}\sin\theta\right)}{\sin\left(k\frac{d}{2}\sin\theta\right)}\frac{\sin\left(kS\frac{K_Rd}{2}\sin\theta\right)}{\sin\left(k\frac{K_Rd}{2}\sin\theta\right)}$$

$$\cdot\frac{\sin\left(k\frac{K_Rd}{2}\sin\theta\right)}{\sin\left(k\frac{d}{2}\sin\theta\right)}.$$

Regardless of the division of the whole array on receiving subapertures, the far field beam is identical to the beam radiated in phase array system for $N = SK_R$

$$|W_{SAR}(\theta)| = \left(\frac{\sin\left(k\frac{Nd}{2}\sin\theta\right)}{\sin\left(k\frac{d}{2}\sin\theta\right)}\right)^2. \tag{22}$$

The far field transmitting/receiving beam pattern for 64 transducers SRA linear array is shown in Fig. 9. The corresponding effective aperture for SRA is shown in Fig. 10. It should be noticed that for this type of SAR the level of diffraction side lobes (Fig. 9) and the effective aperture (Fig. 10) are identical to that of *phase array*.

The effective aperture is given by

$$AP_{\text{eff}\,SRA}(k) = \sum_{i=0}^{S-1}(\mathbf{w}_T^i * \mathbf{w}_R^i)(k),$$
$$k = 1, \ldots 2N-1, \tag{23}$$

where

$$\mathbf{w}_T^i = [1, \ldots, 1],$$
$$\mathbf{w}_R^n = [0, \ldots, 0, A_n, A_{n+1}, \ldots, A_{n+K_R-1}, 0, \ldots, 0],$$
$$n = iK_R + 1.$$

For uniform apodization A_n, $A_{n+1}, \ldots, A_{n+K_R-1} = 1$.

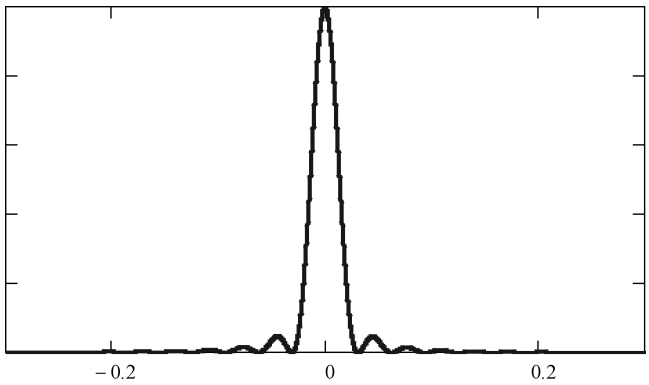

Fig. 9. Far field transmit/receive response $W(\theta)$ for a SRA, linear array of 64 elements, receiving subaperture $K_R = 16$ (four receiving subapertures).

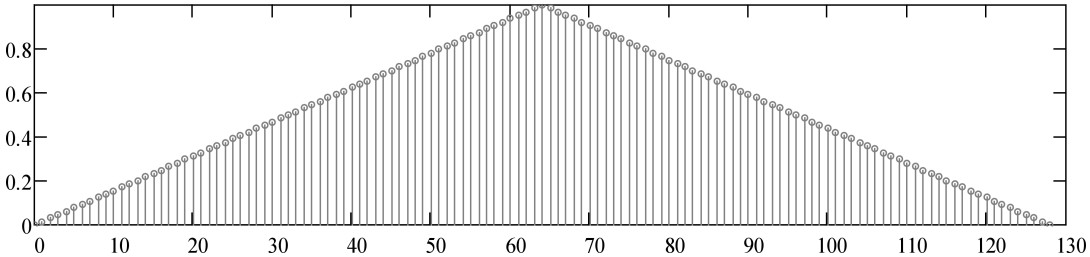

Fig. 10. SRA effective aperture 64 elements SRA, receiving subaperture $K_R = 16$ (four receiving subapertures). The effective aperture of this SAR is identical to that of *phase array*.

6. Synthetic Transmit Aperture STA

In Synthetic Transmit Aperture STA we can distinguish two different systems. The first, in which single array transducers are transmitting the scanning pulses, and then all array elements receive the echoes. Focusing is done during transmission and reception providing high frame rate.

Very large memory is required to record all echoes. In a standard beam forming array with N elements, N echo lines are recorded by each array element involved in the image line imaging (Holm, Yao, 1997; 1999). In STA N^2 have to be stored in order to effectively synthesize and reconstruct the image.

If the elements are grouped into K_T transmitting subarrays elements then the required size of memory decreases proportionally to N/K_T. A certain modification of the STA is the choice of sparse transmitting subarray (Behar, Adam, 2005; Nikolov, Behar, 2005a; 2005b; Lockwood *et al.*, 1996; 1998; Lockwood, Foster, 1995).

In STA the transmitting subapertures are similar to those in M-SAF. Let us divide the aperture $L = Nd$ on S subapertures of length $K_T = N/S$ elements each, $(m = 1, \ldots, K_T)$.

After taking into account only the delays corresponding to the angle steering of the beam, shape in the far field takes the form

$$W_{STA}(\theta) = \sum_{n=0}^{N-1} e^{-jknd\sin\theta} \sum_{i=0}^{S-1} e^{-jkiK_T d\sin\theta} \sum_{m=0}^{K_T-1} e^{-jkmd\sin\theta}. \tag{24}$$

The amplitude of the lateral distribution of the beam is:

$$|W_{STA}(\theta)| = \frac{\sin\left(k\frac{N}{2}d\sin\theta\right)}{\sin\left(k\frac{d}{2}\sin\theta\right)} \frac{\sin\left(k\frac{SK_Td}{2}\sin\theta\right)}{\sin\left(k\frac{K_Td}{2}\sin\theta\right)} \cdot \frac{\sin\left(k\frac{K_Td}{2}\sin\theta\right)}{\sin\left(k\frac{d}{2}\sin\theta\right)} = \left[\frac{\sin\left(k\frac{N}{2}d\sin\theta\right)}{\sin\left(k\frac{d}{2}\sin\theta\right)}\right]^2. \tag{25}$$

It is clear that STA far field response is identical with the field generated by *phase array* regardless of the subapertures' number.

The effective aperture of STA array is given by expression

$$AP_{\text{eff}\,STA}(i) = \sum_{k=1}^{N-K_T+1} \left(\mathbf{w}_T^k * \mathbf{w}_R^k\right)(i), \quad i = 1, \ldots, 2N-1, \tag{26}$$

where

$$\mathbf{w}_T^k = [0, \ldots, 0, A_k, A_{k+1}, \ldots, A_{k+K_T-1}, 0, \ldots, 0],$$

$$\mathbf{w}_R^k = [1, \ldots, 1],$$

for uniform apodization each non-zero element of $\mathbf{w}_T^k$ is equal 1.

7. Summary

In the review three different synthetic apertures schemes are discusses. The worse quality of imaging is obtained using SAF, which is the simplest of all three methods. The gratings lobes appear in the image field two times often than the phase array. In order to minimize this effect the distance (pitch) between adjacent transducers should reduce to $d = \lambda/4$. Already $d = \lambda/2$ is rather difficult technological problem so the design of half of that pitch is not rational. And obviously small aperture of individual sources results in low image quality. In M-SAF the transmitting subaperture increases several times, in addition to improved lateral resolution the signal/noise ratio greatly increases.

Even higher resolution, and in particular the contrast dynamics is obtained in SRA, where the entire array acts as a transmitting aperture, and the synthesis is carried out on the receiving side. The STA, the last of discussed synthetic apertures techniques, enables the image reconstruction with quality similar to that obtained by phase array however with much faster frame rates and focusing practically at each image pixel.

Appendix

As it is known, the convolution, algebraically, is the same operation as multiplying the polynomials with coefficients being the elements of vectors $\mathbf{u}$ and $\mathbf{v}$, starting from the 0th order coefficient (constant).

In the Appendix it is shown that the convolution of two vectors can be rewritten using the linear algebra in a different way than by the use of the well-known concept of *circulant matrix* and *circular convolution*. The algebraic approach given below does not require any assumption about the periodicity of the initial data. Our approach to discrete convolution is to define the convolution operator as a matrix of the third order, which multiply from the both sides by two vectors forms a vector being their convolution.

Let us introduce some notion. The orthonormal basis of the N-dimensional vector space: $\mathbf{e}^1, \mathbf{e}^2, \ldots, \mathbf{e}^N$ is a set of N linearly independent orthonormal vectors, so $(\mathbf{e}^i \cdot \mathbf{e}^j) = \delta_{ij}$, where "$\cdot$" denotes internal product, i.e. scalar product of vectors.

Vectors $\mathbf{u}$ and $\mathbf{v}$ are written in the basis as follows

$$\mathbf{u} \equiv \sum_{i=1}^{N} \left(\mathbf{u} \cdot \mathbf{e}^i\right) \mathbf{e}^i = \sum_{i=1}^{N} u_i \mathbf{e}^i,$$

$$\mathbf{v} \equiv \sum_{i=1}^{N} \left(\mathbf{v} \cdot \mathbf{e}^i\right) \mathbf{e}^i = \sum_{i=1}^{N} v_i \mathbf{e}^i,$$

where u_i, v_i are i-th coordinates of vectors $\mathbf{u}$ and $\mathbf{v}$, respectively. The scalar product of vectors has the value: $\mathbf{u} \cdot \mathbf{v} = \sum_{i=1}^{N} \mathrm{u_i v_i}$.

From two vectors belonging to the same N-dimensional vector space, *outer vector multiplication* is the second rank tensor, called vector's dyad:

$$\mathbf{M} \equiv \mathbf{u} \otimes \mathbf{v} \equiv \sum_{i=1}^{N} \sum_{j=1}^{N} u_i v_j \left(\mathbf{e}^i \otimes \mathbf{e}^j\right),$$

where the set $\Xi = \left\{\left(\mathbf{e}^i \otimes \mathbf{e}^j\right),\ i = 1..N,\ j = 1...N\right\}$ forms the basis of $N \times N$ dimensional linear space of second rank tensors. The (i, j) element of the tensorial basis in the matrix representation is the matrix with 0 element in every place except lying on the cross section of row and column, i.e.:

$$\mathbf{e}^i \otimes \mathbf{e}^j \equiv \begin{bmatrix} 0 & \cdots & 0 & \cdots & 0 \\ \vdots & & \vdots & & \vdots \\ 0 & \cdots & 1 & \cdots & 0 \\ \vdots & & \vdots & & \vdots \\ 0 & \cdots & 0 & \cdots & 0 \end{bmatrix} \leftarrow i\text{-th row, } j\text{-th column.}$$

The numerical representation of the vector dyad is the quadratic NxN dimensional matrix, formed from vectors coordinates as follows:

$$M_{ij} \equiv u_i v_j \equiv \begin{bmatrix} u_1 v_1 & u_1 v_2 & \cdots & u_1 v_N \\ u_2 v_1 & u_2 v_2 & \cdots & u_2 v_N \\ \vdots & \vdots & & \vdots \\ u_N v_1 & u_N v_2 & \cdots & u_N v_N \end{bmatrix}.$$

Anti-diagonals, see Wen Yan and Tin-Yau Tam (2013), are elements of matrix lying on lines from right up to left down, in perpendicular direction to classical diagonals which are lines from left up to right down. The number of anti-diagonals is equal to $2N-1$ (the same as diagonals) and the elements of k-th anti-diagonal read as: $u_j v_{k-j+1}$ for $j \in \langle j^{\min} j^{\max} \rangle$, where $j^{\min} = \max(1, k+1-N)$ and $j^{\max} = \min(k, N)$, $k = 1, \ldots, 2N-1$. *Convolution of two vectors with the same finite length* N forms vector $\mathbf{w}$ of length $2N-1$ with elements being sums of elements lying on anti-diagonals:

$$w_k = \sum_{j=j^{\min}}^{j^{\max}} u_j v_{k-j+1}, \qquad k = 1, \ldots, 2N-1.$$

For vectors

$$\mathbf{u} = (u_1, u_2, \ldots, u_M) \quad \text{and} \quad \mathbf{v} = (v_1, v_2, \ldots, v_N)$$

their outer product $\mathbf{u} \otimes \mathbf{v}$ is defined as $M \times N$ matrix $\mathbf{A}$ obtained by multiplying each element of $\mathbf{u}$ by each element of $\mathbf{v}$:

$$A_{ij} \equiv u_i v_j \equiv \begin{bmatrix} u_1 v_1 & u_1 v_2 & \ldots & u_1 v_N \\ u_2 v_1 & u_2 v_2 & \ldots & u_2 v_N \\ \vdots & \vdots & & \vdots \\ u_M v_1 & u_M v_2 & \cdots & u_M v_N \end{bmatrix}.$$

Now, the *convolution of the vectors* $\mathbf{w} = \mathbf{u} * \mathbf{v}$ *with different finite length* ($M = \mathrm{length}\,(\mathbf{u})$, $N = \mathrm{length}\,(\mathbf{v})$) is the vector of length $M+N-1$, where k-th element has the form:

$$w_k = \sum_{j=j^{\min}}^{j^{\max}} u_j v_{k-j+1}, \qquad k = 1, \ldots, M+N-1.$$

The summation is done over all the values of j which lead to legal subscripts for u_j and v_{k-j+1} specifically j changes from value $j^{\min} = \max(1, k+1-N)$ to $j^{\max} = \min(k, M)$.

In particular, if we have two vectors with coordinates [1, 1, 1] and [1, 2, 1, 1] then their outer matrix product and convolution (sum of elements lying on anti-diagonals) have the forms:

$$A_{ij} = \begin{bmatrix} 1 & 2 & 1 & 1 \\ 1 & 2 & 1 & 1 \\ 1 & 2 & 1 & 1 \end{bmatrix}, \qquad \mathbf{w} = (1, 3, 4, 4, 2, 1).$$

The set $\Xi = \left\{\left(\mathbf{e}^i \otimes \mathbf{e}^j\right),\ i = 1..M,\ j = 1...N\right\}$ forms the $M \times N$ dimensional basis of linear space of second rank tensors. The (i, j) element of the tensorial basis in the matrix representation is the matrix with 0 elements in every position except the position lying on the cross section of row and column, where the element has value equal to 1, i.e.:

$$\mathbf{e}^i \otimes \mathbf{e}^j \equiv \begin{bmatrix} 0 & \cdots & 0 & \cdots & 0 \\ \vdots & & \vdots & & \vdots \\ 0 & \cdots & 1 & \cdots & 0 \\ \vdots & & \vdots & & \vdots \\ 0 & \cdots & 0 & \cdots & 0 \end{bmatrix} \leftarrow \begin{array}{l} 1 \text{ on the position:} \\ i\text{-th row, } j\text{-th column.} \end{array}$$

Now, we introduce the sequence of second rank tensors $\mathbf{J}^k$ for $k = 1, \ldots, M+N-1$ as follows

$$\mathbf{J}^k = \sum_{j=j^{\min}}^{j^{\max}} \mathbf{e}^j \otimes \mathbf{e}^{k-j+1},$$

$$\mathbf{J}^3 = \begin{bmatrix} 0 & 0 & 1 & 0 & \cdots & 0 \\ 0 & 1 & 0 & 0 & \cdots & 0 \\ 1 & 0 & 0 & 0 & \cdots & 0 \\ 0 & 0 & 0 & 0 & \cdots & 0 \\ \vdots & \vdots & \vdots & \vdots & \ddots & \vdots \\ 0 & 0 & 0 & 0 & \cdots & 0 \end{bmatrix},$$

where $j^{\min} = \max(1, k+1-N)$ to $j^{\max} = \min(k, M)$. Let us notice that in the matrix representation the only non-zero elements (equal to 1) are lying on the k-th anti-diagonal.

The sequence $\{\mathbf{J}^k\}$, $k = 1, \ldots, M+N-1$ of second rank tensors can be identified with 3 dimensional block – 3D matrix (or third order tensor) – formed from 2 dimensional $M \times N$ matrices and can be rewritten as:

$$J^k_{\alpha P}, \quad k = 1, \ldots, M+N-1,$$

$$\alpha = 1, \ldots, M, \quad P = 1, \ldots, N.$$

Convolution is just the classical multiplication of the 3D matrix by two vectors and can be calculated as follows:

$$w_k = \sum_{\alpha=1}^{M} \sum_{P=1}^{N} J^k_{\alpha P} u_\alpha v_P, \qquad k = 1, \ldots, M+N-1.$$

For every fixed $k = 1, \ldots M+N-1$, the second rank tensors $\mathbf{J}^k$ is symmetric and the above convolution follows directly that the convolution operation is commutative, i.e.

$$\mathbf{w} = \mathbf{u} * \mathbf{v} = \mathbf{v} * \mathbf{u}.$$

Moreover, 3D matrix $\mathbf{J} = (J^k_{\alpha P})$ (general definition of 3D matrix given in cf. Kilmer and Moravitz (2004), Gnang Edinah *et al.* (2011), can be named as the *convolution tensor or 3D convolution operator* because it is an operator acting on two given vectors and resulting in the vector being their convolution:

$$\mathbf{u}\mathbf{J}\mathbf{v}^{\mathrm{T}} = \mathbf{u} * \mathbf{v}.$$

Let us summarize the above result and let us notice that the calculation of the convolution of two vectors with finite length based on the last formula doesn't involve the *FFT* and *inverse FFT*, contrary to the method based on *circular convolution* notion.

References

1. Behar V., Adam D. (2005), *Optimization of sparse synthetic transmit aperture imaging with coded excitation and frequency division*, Ultrasonics, **43**, 777–788.
2. Burckhardt C.B., Grandchamp P.A., Hoffmann H. (1974), *An experimental 2MHz synthetic aperture sonar system intended for medical use*, IEEE Trans. Son. Ultrason., **21**, 1, 1–6.
3. Chiao R.Y., Thomas L.J. (1996), *Aperture formation on reduced-channel arrays using the transmit-receive apodization matrix*, IEEE Proc. Ultrasonics Symposium, 1567–1571.
4. Flaherty J.J., Erikson K.R., Lund V.M. (1967), *Synthetic aperture ultrasound imaging systems*, United States Patent, US 3, 548, 642.
5. Gnang Edinah K., Elgammaly A., Retakhz V. (2011), *A Spectral Theory for Tensors*, preprint, arXiv:1008.2923v4 [math.SP] 3 Nov 2011.
6. Hansen J.M., Jensen J.A. (2012), *Compounding in synthetic aperture imaging*, IEEE Trans. Ultrason. Ferroelectr. Freq. Control., **59**, 9, 2054–65.
7. Holm H., Yao H. (1997), *Improved frame rate with synthetic transmit aperture imaging using prefocused subapertures*, Proc. IEEE Ultrason. Symp., Toronto.
8. Holm S., Yao H. (1999), *Method and apparatus for synthetic transmit aperture imaging*, US patent No 5.951.479, Sep. 14.
9. Jensen J.A., Nikolov S.I., Gammelmark K.L., Pedersen M.H. (2006), *Synthetic aperture ultrasound imaging*, Ultrasonics, **44**, 5–15.
10. Karaman M., Li Pai-Chi, O'Donnell M. (1995), *Fellow, IEEE Synthetic Aperture Imaging for Small Scale Systems*, IEEE Transactions On Ultrasonics, Ferroelectrics, and Frequency Control, **42**, 3, 429–442.
11. Karaman M., Bilge H., O'Donnell M. (1998), *Adaptive multi-element synthetic aperture imaging with motion and phase aberration correction*, IEEE Trans. Ultrason. Ferroelec. Freq. Contr., **45**, 4, 1077–1086.
12. Karaman M., O'Donnell M. (1998), *Subaperture processing for ultrasonic imaging*, IEEE Trans. Ultrason. Ferroelec. Freq. Contr., **45**, 126–135.
13. Karwat P., Klimonda Z., Seklewski M., Lewandowski M., Nowicki A. (2010), *Data Reduction Method for Synthetic Transmit Aperture Algorithm*, Archives of Acoustics, **35**, 4, 635–642.
14. Kilmer M.E., Moravitz Martin C.D. (2004), *Decomposing a tensor*, SIAM News, **37**, 9.
15. Kim D., Park J., Cho J., Song T.K., Yoo Y. (2012), *New synthetic aperture imaging technique with dynamic apodization window*, Proc. SPIE, Medical Imaging.
16. Kortbek J., Jensen J.A., Gammelmark K.L. (2013), *Sequential beamforming for synthetic aperture imaging*, Ultrasonics, **53**, 1–16.
17. Lockwood G.R., Li P.C., O'Donnell M., Foster F.S. (1996), *Optimizing the radiation pattern of sparse periodic linear arrays*, IEEE Trans. Ultrason., Ferroelec. and Freq. Cont., **43**, 1, 4–12.
18. Lockwood G.R., Talman J.R., Brunke S.S. (1998), *Real-time 3-D ultrasound imaging using sparse synthetic aperture beamforming*, IEEE Trans. Ultrason. Ferroelec. Freq. Contr., **45**, 980–988.

19. Lockwood G.R., Foster F.S. (1995), *Design of sparse array imaging systems*, Proc. Ultrasonics Symposium, 1237–1243.

20. Mosey S.A., Charlton P.C., Well I.A. (2013), *Modified Synthetic Aperture Focusing Technique Utilising the Spatial Impulse Response of the Ultrasound*, NDT.net e-Journal.

21. Nikolov M., Behar V. (2005a), *Analysis and Optimization of Medical Ultrasound Imaging Using the Effective Aperture Approach*, Cybernetics and Information Technologies, **5**, 2, Sofia, Bulgarian Academy of Sciences, 53–68.

22. Nikolov M., Behar V. (2005b), *Analysis and Optimization Of Synthetic Aperture Ultrasound Imaging Using The Effective Aperture Approach*, International Journal, Information Theories and Applications, **12**, 3, 257–264.

23. Nock L.P., Trahey G.E. (1992), *Synthetic receive aperture imaging with phase correction formotion and for tissue inhomogeneities. Part I: Basic principles*, IEEE Trans. Ultrason. Ferroelec. Freq. Contr., **39**, 4, 489–495.

24. O'Donnell M., Thomas L.J. (1992), *Efficient synthetic aperture imaging from a circular aperture with possible application to catheter-based imaging*, IEEE Trans. Ultrason. Ferroelec. Freq. Contr., **39**, 366–380.

25. Trahey G.E., Nock L.P. (1992), *Synthetic receive aperture imaging with phase correction for motion and for tissue inhomogeneities. Part II: Effects of and correction for motion*, IEEE Trans. Ultrason. Ferroelec. Freq. Contr., **39**, 4, 496–501.

26. Trots I., Nowicki A., Lewandowski M. (2008), *Laboratory setup for synthetic aperture ultrasound imaging*, Archives of Acoustics, **33**, 4, 573–580.

27. Walker W.F., Trahey G.E. (1994), *Real-time synthetic receive aperture imaging: experimental results*, Proc. IEEE Ultrasonics Symposium.

28. Wen Yan, Tin-Yau Tam (2013), *Anti-diagonals of symmetric and skew symmetric matrices with prescribed eigenvalues*, Linear Algebra and its Applications, **438**, 1446–1453.

29. Yao H. (1997), *Synthetic Aperture Methods for Medical Ultrasonic Imaging*, Ph.D. Thesis, University of Oslo, Norway.

30. Ylitalo J.T. (1996), *On the signal-to-noise ratio of a synthetic aperture ultrasound imaging method*, Europ. J. Ultras., **3**, 277–281.